Optical analog of Magnus effect

A. V. Dugin, Ya. B. Zel'dovich, N. D. Kundikova, and V. S. Liberman

Chelyabinsk State Technical University

An optical analog of the Magnus effect, manifested in rotation of the speckle pattern of circularly polarized light emerging from an optical fiber upon reversal of the circulation, is theoretically predicted and experimentally observed. The effect can be interpreted as the result of photon spin-orbit interaction in an inhomogeneous medium.

INTRODUCTION

Consider a sphere revolving around its axis and falling in air. The Magnus effect deflects it from the vertical in the direction of its revolution. A circularly polarized photon multiply reflected in a graded-index waveguide can be likened to the motion of body revolving in air. Will the photon be deflected from its initial trajectory in this case?

More than 50 years ago S. M. Rytov[1] and V. V. Vladimirskiĭ[2] calculated the rotation of the plane of polarization of a geometric-optics beam with nonzero twist of the trajectory. Recently such a rotation was observed in a single-mode fiber[3] and interpreted in terms of the Berry geometric phase.[4]

We consider in the present paper an effect that is in some respect the inverse: rotation of a speckle picture in a multimode fiber when the circular polarization is reversed from left- to right-hand. In the language of quantum mechanics this effect can be regarded as the result of interaction between the orbital momentum of the photon and its spin (polarization).

We have published recently some preliminary theoretical and experimental results.[5,6]

THEORY

Consider propagation of light in an axisymmetric fiber with the following profile of the refractive index $n(r)$

$$n^2(r) = n_{co}^2[1 - 2\Delta S(r/\rho)].\qquad(1)$$

Here $r = |\mathbf{r}|$, where $\mathbf{r}(x,y)$ is the radius-vector of a section point, ρ is the radius of the core, n_{c0} and n_{c1} are the refractive indices of the core and the sheath, respectively, $\Delta = (n_{c0}^2 - n_{c1}^2)/2n_{c0}^2 \approx \delta n/n_{c0} \ll 1$ is indicative of the height of the profile, where $\delta n = n_{c0} - n_{c1}$, $S(r/\rho)$ is a function of the profile, with $S(0) = 0$ and $S(1) = 1$.

In the paraxial approximation corresponding to the simplified wave equation, the polarization does not affect the diffraction. Since the refractive indeed is homogeneous, the spatial structure of the field and its polarization are interrelated. The polarization correction to the propagation constant of the mode $\mathbf{e}(r)\exp(i\beta z)$ takes in first-order approximation the form [see Ref. 7, Chap. 32, Eq. (32.24)]:

$$\delta\beta = -\frac{(2\Delta)^{1/2}\rho}{2V}\frac{\int(\nabla_\perp \mathbf{e}_\perp)(\mathbf{e}_\perp^* \cdot \nabla_\perp \ln n^2(\mathbf{r}))d^2\mathbf{r}}{\int \mathbf{e}_\perp^* \cdot \mathbf{e}_\perp d^2\mathbf{r}}.\qquad(2)$$

Here $\mathbf{e}(\mathbf{r}) = \mathbf{e}_\perp(\mathbf{r}) + e_z(r)\mathbf{e}_z$, $\nabla_\perp = \partial/\partial\mathbf{r} = \mathbf{e}_x(\partial/\partial x) + \mathbf{e}_y(\partial/\partial y)$, $V = \rho k n_{c0}(2\Delta)^{1/2}$ is a dimensionless param-

eter, $V \gg 1$ for a multimode fiber, $k = 2\pi/\lambda$, and λ is the wavelength of the light in air.

Since the fiber is axisymmetric, we can calculate the polarization corrections $\delta\beta$ by choosing in the zeroth (uncoupled) approximations the modes to be the functions

$$\mathbf{e}_{m,N}^{\pm}(r,\varphi) = 2^{-1/2}(\mathbf{e}_x \pm i\mathbf{e}_y)\exp(im\varphi)F_{|m|,N}(r),\qquad(3)$$

corresponding to right- and left-hand circular polarization and to angular-momentum values $m = 0, \pm 2, \pm 3, \pm 4, \ldots$ Here $x = r\cos\varphi$, $y = r\sin\varphi$, $F_{|m|,N}(r)$ is a radial function, $N = 0, 1, \ldots$ is the radial quantum number. It was shown in Ref. 7 that for $m \neq \pm 1$ it is just these modes which are the corresponding basis for diagonalizing the perturbations of grad n.

It should be noted that in our approximation the laser radiation propagating in the fiber conserves its circular (right- or left-hand) polarization. The only exception may be the modes with $m = +1$ or $m = -1$, whose contribution will henceforth be neglected.

In the case of a fiber with a parabolic refractive-index profile, $S(r/\rho) = (r/\rho)^2$ for $r \leqslant \rho$, an analytic expression can be obtained for the polarization corrections. The radial functions take in this case the form

$$F_{|m|,N}(r) = (r/\rho)^{|m|}L_N^{|m|}(Vr^2/\rho^2)\exp(-Vr^2/\rho^2),\qquad(4)$$

where $L_N^{|m|}$ are generalized Laguerre polynomials. It follows then from (2) that

$$\delta\beta_m^{\pm} = -\frac{\Delta}{2\pi\rho^2}n(1\pm m).\qquad(5)$$

It is interesting to note that the correction (5) does not depend on the radial quantum number N, a specific feature of a fiber with a parabolic refractive-index profile.

Assume that right-polarized light is fed to the input of the fiber. The field distribution at the exit from the fiber is then

$$\mathbf{E}^+(r,\varphi,z) = \frac{\mathbf{e}_x + i\mathbf{e}_y}{2^{1/2}}\sum\sum C_{m,N}e^{im\varphi}F_{|m|,N}(r)$$

$$\times \exp[iz(\beta_{mN} + \delta\beta_{mN}^+)].\qquad(6)$$

A similar expression can be obtained for left-circularly-polarized light.

Consider the most interesting case, when left- and right-polarized light with equal mode structure $C_{m,N}$ is fed in succession to the input of the fiber. It would be of interest to compare the field and (or) intensity distributions for $(\mathbf{e}_x + i\mathbf{e}_y)$ and $(\mathbf{e}_x - i\mathbf{e}_y)$ in one and the same cross section z. The qualitative analogy with the mechanical Magnus effect suggests that these distributions will be similar but

somewhat rotated relative to one another around the fiber axis. This hypothesis is easiest to verify theoretically in the case of a parabolic refractive-index profile. We choose $\delta\beta_{mN}^{\pm}$ from (5), then

$$\mathbf{E}^{\pm}(r, \varphi, z) = \frac{\mathbf{e}_x \pm i\mathbf{e}_y}{2^{1/2}} \sum\sum C_{m,N}$$

$$\times \exp[im(\varphi \pm \varkappa z)] F_{|m|,N}(r) \exp(iz\beta_{mN}), \qquad (7)$$

where

$$\varkappa = \frac{\Delta}{2\pi\rho^2 n}\lambda. \qquad (8)$$

It is seen from (7) that the $|\mathbf{E}^{\pm}(r,\varphi,z)|^2$ distributions are similar, but displaced from one another by an angle

$$\varphi_+ - \varphi_- = 2\varkappa z. \qquad (9)$$

Let us examine the mechanical analogy with the rotation of a ping-pong ball, and replace the sign of its rotation by that of the rotation vector of the electric vector of a light wave in the given cross section. The rotation of the sphere about its own axis is manifested by deflection of its trajectory after many reflections from a rough internal wall of an axisymmetric "ball guide." The sign of the deflection of the ball agrees then with the sign of our optical effect.

No analytical solution can be obtained for a fiber with a stepped profile of the refractive index. The modes and the corresponding corrections (2) were therefore obtained numerically for specific fiber parameters: $n = 1.5$, $\delta n = 0.006$, $\lambda = 0.63\,\mu$m (He–Ne laser), $2\rho = 200\,\mu$m.

It is important to note that in the general case of a refractive index with a nonparabolic profile the dependence of $\beta_{mM}^+ - \beta_{mN}^-$ on m and N is complicated. The intensity distributions $|E^+(r,\varphi,z)|^2$ and $|E^-(r,\varphi,z)|^2$ will therefore not be the same even if the mode amplitudes at the input to the fiber are identical. One can hope, however, that these distributions will remain similar over a certain propagation length, but one will be turned away from the other by an angle of the order of (9).

The radial functions (2) for a fiber with a stepped refractive-index profile are given by
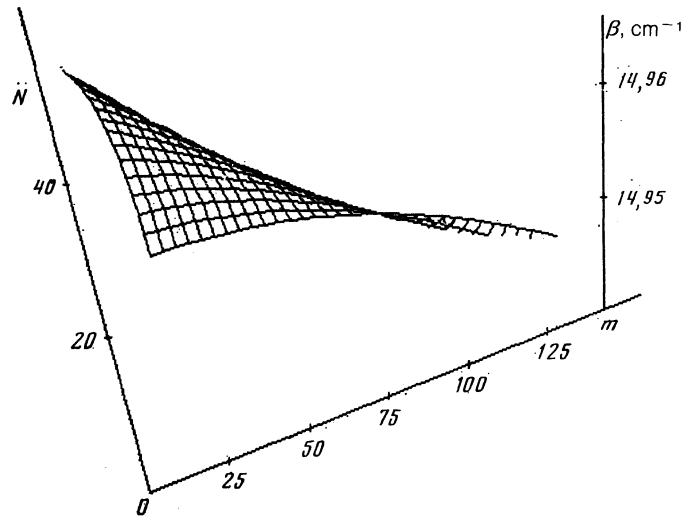
FIG. 1. Dependences of propagation constants on the mode indices, calculated in the scalar approximation for a fiber with stepped refractive-index profile and with the following parameters: $2\rho = 200\,\mu$m, $n_{co} = 1.5$, $\delta n = 0.006$.

$$e_{m,N}^{\pm}(r, \varphi) = \frac{\mathbf{e}_x \pm i\mathbf{e}_y}{2^{1/2}} e^{im\varphi} J_{|m|}(Ur), \quad r/\rho < 1, \qquad (10a)$$

$$e_{m,N}^{\pm}(r, \varphi) = \frac{\mathbf{e}_x \pm i\mathbf{e}_y}{2^{1/2}} e^{im\varphi} K_{|m|}(Wr), \quad r/\rho > 1. \qquad (10b)$$

Here $J_{|m|}$ and $K_{|m|}$ are Bessel and Macdonald functions, respectively, while U and W ($V^2 = W^2 + U^2$) are determined from the equation

$$U\frac{J_{|m|+1}(Ur)}{J_{|m|}(Ur)} = W\frac{K_{|m|+1}(Wr)}{K_{|m|}(Wr)}. \qquad (11)$$

The polarization corrections are, in accordance with (2),

$$\delta\beta_{|m|,N}^+ = \delta\beta_{-|m|,N}^- = \frac{(2\Delta)^{1/2}}{2V\rho}\frac{WU^2}{V^3}\frac{K_{|m|}(Wr)}{K_{|m|+1}(Wr)}, \qquad (12a)$$

$$\delta\beta_{|m|,N}^- = \delta\beta_{-|m|,N}^+ = \frac{(2\Delta)^{1/2}}{2V\rho}\frac{WU^2}{V^3}\frac{K_{|m|}(Wr)}{K_{|m|-1}(Wr)}. \qquad (12b)$$
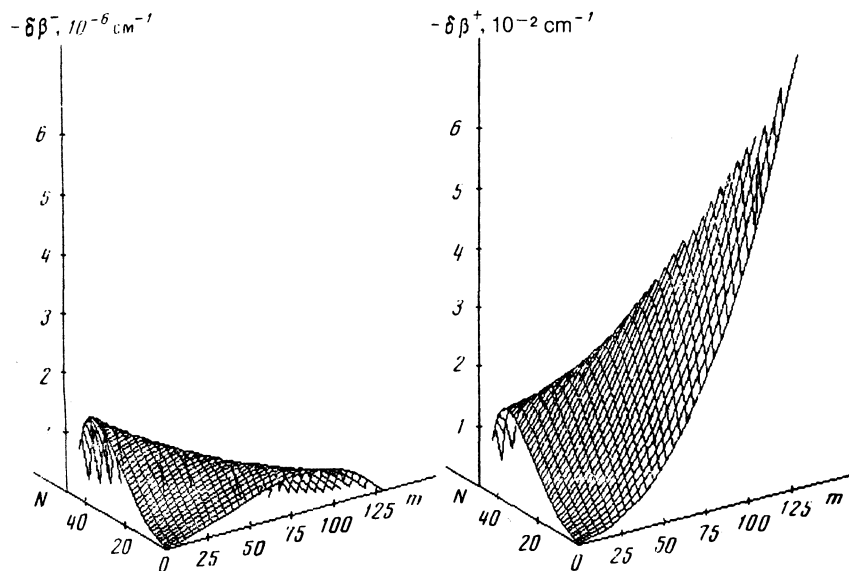
FIG. 2. Dependences of the polarization corrections to the mode-indices propagation constants, calculated in the scalar approximation for a fiber with stepped refractive-index profile and with parameters $2\rho = 200$ m, $n_{co} = 1.5$, and $\delta n = 0.006$.
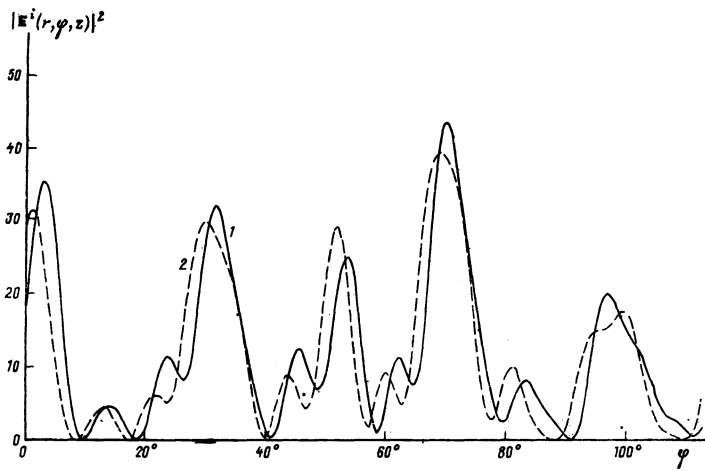
FIG. 3. Angular distribution of speckle pictures $|E^i(r,\varphi,z)|^2$ of right ($i =$ "$+$") (1) and left ($i =$ "$-$") (2) circularly polarized light for a fiber $z = 96$ cm long at a radius $r = \rho/2$.

These equations were used for a numerical simulation of the physical experiment.

COMPUTER EXPERIMENT

Figures 1 and 2 show the dependences of the propagation constants and polarization corrections on the mode indices m and N. It is seen from Fig. 1 that only modes with $m \leqslant 129$ and $N \leqslant 44$ can propagate in our fiber. For the numerical simulation, however, we used only modes with $m \leqslant 60$ and $N \leqslant 20$, corresponding to the speckle picture observed in experiment. The complex amplitudes $C_{m,N}$ for the actual realization of the speckle picture in (6) were chosen using a random-number generator. Figure 3 shows, for left- and right-hand circular polarizations, the angular distributions of the actual realization of the speckle-picture $|E^{\pm}(r,\varphi,z)|^2$ at a fixed radius. It is easily seen from Fig. 3 that when the sign of the circular polarization is reversed the entire picture shifts in angle (is rotated) as a unit, retains the main features, and is only insignificantly altered. The angular displacement is in this case 1.5.°

To separate the pure rotation from all the changes in the speckle-picture the pure rotation, we calculated the correla-

tion functions

$$K_{ij}(r, \psi, z) = \int I_i(r, \varphi, z)I_j(r, \varphi+\psi, z)\,d\varphi,$$

$$I_i(r, \varphi, z) = |\mathbf{E}^i(r, \varphi, z)|^2, \quad i=+, -; \quad j=+, -.$$

(13)

Averaging over a statistical ensemble was consequently replaced by averaging over the angle φ in an interval $0 < \varphi < 2\varphi_0$, $\varphi_0 \gg \pi/m_{\max}$, $2\varphi_0 = 360°$. Our effect is manifested by a sharp maximum of the correlation function $K_{+-}(\psi)$ at a certain value $\psi_0 \neq 0$, which is in fact the "rotation angle" $\psi_0 = \varphi_+ - \varphi_-$.

Figure 4 shows the autocorrelation function for left-hand circular polarization $K_{--}(\psi)$ and the correlation functions $K_{+-}(\psi)$ for different radii and for different realizations. Figure 5 shows the correlation functions for different fiber lengths. Just as assumed, the correlation function has a clearly pronounced maximum at an angle $\psi_0 \neq 0$, which is proportional to the length and equals 1.5° at $z = 96$ cm irrespective of the radius and of the actual realization. Interestingly, the correlation-function modulation depth corresponds to the case of Gaussian statistics.
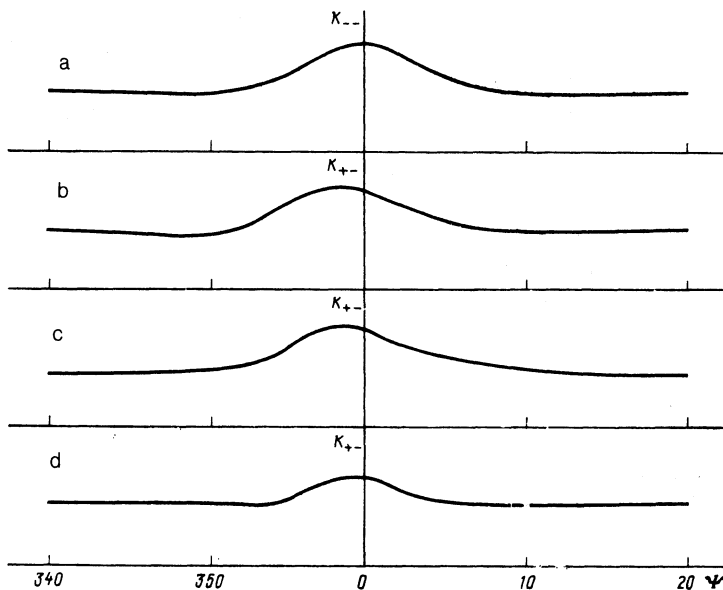
FIG. 4. Dependence of the autocorrelation function $K_{--}(r,\psi,z)$ (a) and of the correlation functions $K_{+-}(r,\psi,z)$ (b,c,d) on the angular shift between the speckle pictures for fibers $z = 96$ cm long and with different radii and realizations a,b,d—$r = \rho/2$; c—$r = 0.8\rho$; a,c,d—first realization; b—second realization.
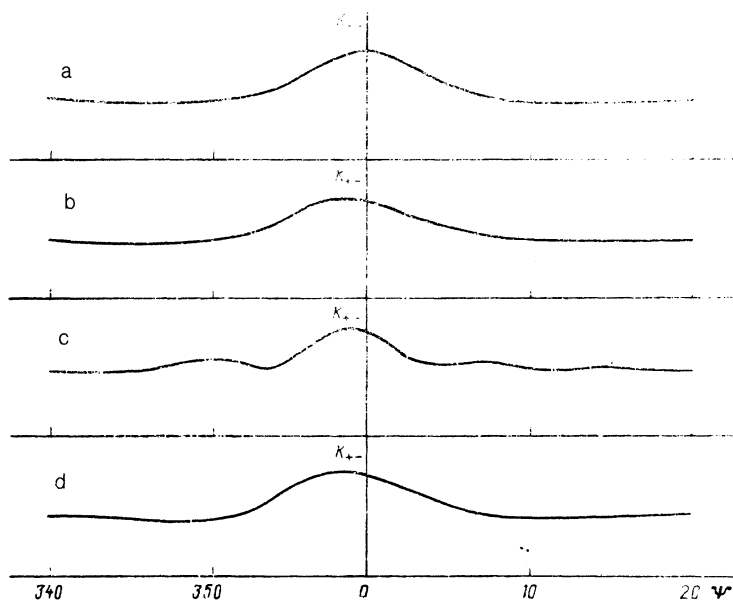
FIG. 5. Dependences of the autocorrelation function $K_{--}(r,\psi,z)$ (a) and of the autocorrelation functions $K_{+-}(r,\psi,z)$ (b,c,d) on the angle shift between the speckle pictures at a radius $r = \rho/2$ for fibers of various lengths: $z = 96$ cm (a,b), $z = 72$ cm (c), and $z = 48$ cm (d).

EXPERIMENT

Unfortunately, we had no graded-index fiber with a parabolic refractive-index profile, in which linear polarization of the light would propagate over reasonable lengths. The experiment was performed on a multimode fiber with a stepped refractive-index profile and with a diameter $2\rho = 200$ μm; the difference $\Delta n = n_{co} - n_{cl} = 0.006$ between the refractive index of the quartz core and the transparent polymer sheath was determined from the limiting angle of light entry into the guide.

Figure 6 shows the experimental setup. Linearly polarized radiation from He–Ne laser 1, of wavelength $\lambda = 0.63$ μm was passed through a Fresnel rhomb 2. The polarization plane was placed relative to the rhomb in such a way that the emerging radiation was circularly polarized. A polarizer 3 made possible linear polarization of any prescribed orientation. The light passed next through a second Fresnel rhomb 4 and was focused by lens 5 on the fiber input 6. The polarization was easily switched from left- and right-hand or back by rotating the polarizer 3 through 90°. The speckle-picture of the radiation emerging from the fiber was observed on a screen with a polar-coordinates grid.

We verified first the polarization properties of our fiber. The polarization stayed linear in a fiber 20–30 cm long, but the hoped-for effect was not observed. The light at the exit from fibers longer than 2 m was strongly depolarized, and reversal of the sign of the circular polarization led to irregular speckle pictures.

In an lightguide approximately one meter long, the lin-ear polarization was for the most part preserved, and an insignificant fraction of depolarized radiation was observed. Regarding this case as the most favorable for observation of the effect, we used subsequently a fiber 96 cm long. And indeed, as theoretically predicted, when the circular polarization changed from left to right, we succeeded in observing a clockwise speckle-picture "spillover," in which the main singularities moved in a circle without changing shape, while the details showed modifications. This can be easily seen from Fig. 7, which shows, for both polarizations, one and the same fragment of the speckle picture observed on the screen. The arrow points to a bright spot with practically no change in form after rotation (just as in the computer experiment, see Fig. 3).

For a more accurate measurement of the "rotation angle" we used an experimental analog of the correlation-functions method. By projecting on a high-contrast positive speckle picture the negative of the same picture through a slide projector, the contrast of the resultant image will be minimal if the coordinate grids are exactly superimposed (Fig. 8a). The smallest mismatch increases the contrast greatly (Fig. 8b). This corresponds approximately to the autocorrelation function shown in Fig. 4. To measure the rotation angle we projected on the positive image of the speckle picture, in left-polarized light, a negative image in light-polarized light and found, by mutual rotation of the images, the position of the minimum contrast. The angle between the axes of the coordinate grids was regarded by as the sought "rotation angle." It was found to be 1.4° for our fiber. In successive searches for the minimum contrast, this angle was duplicated with 0.5° accuracy.
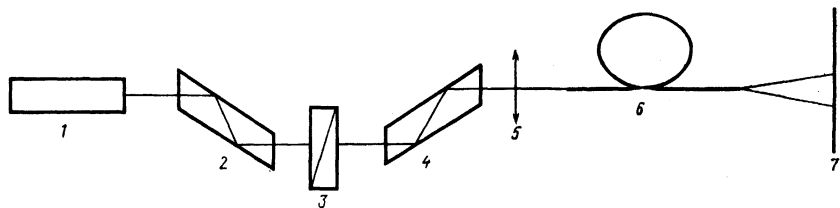
FIG. 6. Experimental setup. 1—He–Ne laser emitting linearly polarized length of wavelength $\lambda = 0.63$ μm; 2, 4—Fresnel rhombs; 3—polarizer; 5—objective; 6—investigated fiber; 7—screen with polar-coordinate grid.
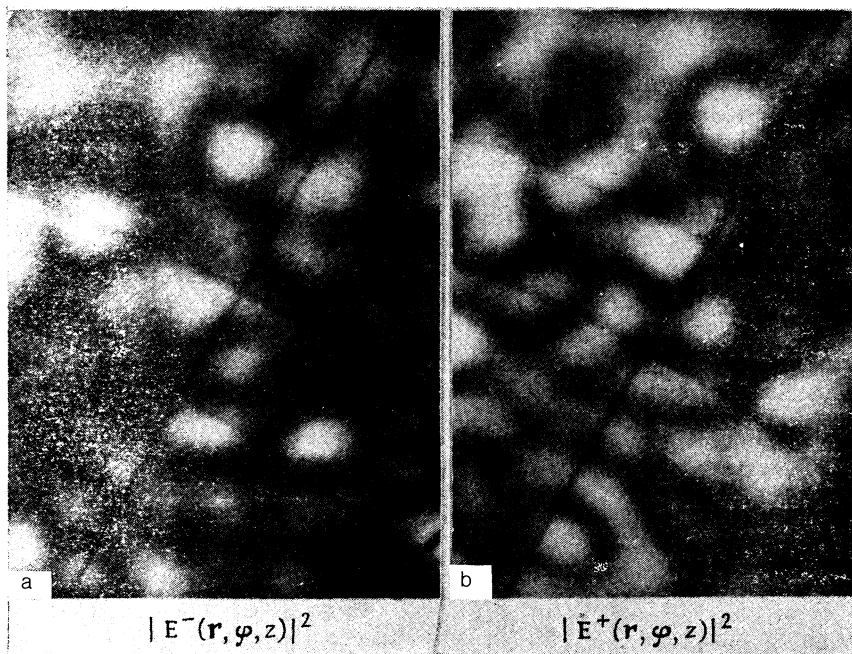
FIG. 7. Fragment of right-hand ($i = $ " $+$ ") and left-hand ($i = $ (" $-$ ") speckle pictures $|E^i(r,\varphi,z)|^2$ observed in experiment on a screen. The arrow points to a spot rotated by reversal of the sign of the circular polarization.

$|E^-(r,\varphi,z)|^2$

$|E^+(r,\varphi,z)|^2$
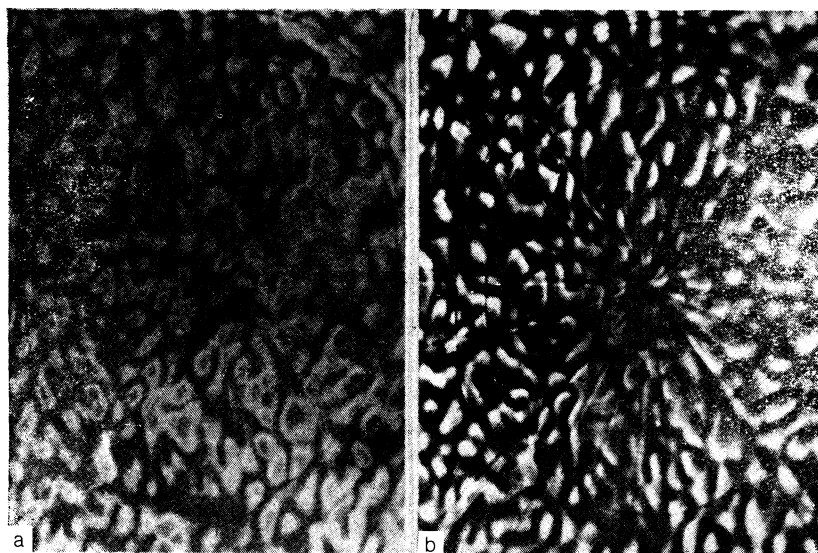
FIG. 8. Negative speckle-picture slide-projected on a positive image of the same speckle picture: a—coordinate grids superimposed; b—coordinate grids rotated relative to each other by an angle $\psi \approx 4°$.

CONCLUSION

The agreement between the theoretically calculated rotation angle $(+1.5 \pm 0.5)°$ with the measured one $(+1.4 \pm 0.5)°$ turned out to be strikingly good. Even an analytic result for a fiber with a parabolic refractive-index profile yields a perfectly acceptable estimate ($+3.3°$) for the magnitude of the effect.

All this convinces us that we have predicted, and observed for the first time ever (in our opinion), an optical analog of the Magnus effect, i.e., rotation of the speckle picture at the exit from a fiber upon reversal of the sign of the circular polarization.

[1] S. M. Rytov, Dokl. Akad. Nauk SSSR 18, 2 (1938).
[2] V. V. Vladimirskii, ibid. 21, 222 (1941).
[3] R. Y. Chiao, A. Tomita, and Y.-S. Wu, in Geometric Phases in Physics, A. Shapere, ed., World Scientific, Singapore, 1989.
[4] M. V. Berry, Proc. Roy. Soc. A 392, 45 (1984).
[5] B. Ya. Zel'dovich and V. S. Liberma, Kvantovaya Elektron. (Moscow) 17, 493 (1990) [Sov. J. Quant. Electron. 20, 427 (1990)].
[6] A. W. Snyder and J. D. Love, Optical Waveguide Theory, Methuen, 1984.

Translated by J. G. Adashko